Self-assembled nanoscale architecture of TiO_2 and application for dye-sensitized solar cells

Motonari Adachi[1,4]
Jinting Jiu[2]
Seiji Isoda[2]
Yasushige Mori[3]
Fumio Uchida[4]

[1]Research Center of Interfacial Phenomena, Faculty of Engineering, Doshisha University, Kyotanabe, Japan; [2]Institute for Chemical Research, Kyoto University Uji, Japan; [3]Department of Chemical Engineering and Materials Science, Faculty of Engineering, Doshisha University, Kyotanabe, Japan; [4]Fuji Chemical Co., Ltd. Hirakata, Japan

Abstract: A single-crystal-like titania nanowire network was successfully synthesized by a surfactant assisted "oriented attachment" mechanism. Highly crystallized titania nanorods have been synthesized by hydrothermal process using block-copolymer F127 with ethylenediamine. It was observed from high resolution TEM image that titanium atoms aligned perfectly in titania anatase structure with no defect. A high light-to-electricity conversion yield (9.3%) was attained by applying these titania nanoscale materials for making an electrode of dye-sensitized solar cells.

Keywords: nanoscale architecture, TiO_2, dye-sensitized solar cells

Introduction

The development of renewable energy resources is an urgent issue to keep high human activity regarding to global environments. Fortunately, the supply of energy from the sun to the earth is gigantic, ie, 3×10^{24} J/year or about 10^4 times more than what mankind consumes currently. One attractive strategy is the development of dye-sensitized solar cells (DSSCs). DSSCs appear to have significant potential as a low cost alternation to conventional p-n junction silicon solar cells. The cell system has already reached conversion efficiencies exceeding 11% (Grätzel 2004, 2005, 2006; Chiba et al 2006). Nevertheless, the energy conversion efficiency of the cells for commercial devices has not yet reached that level, which provides a lower cost than that of conventional methods of electricity generation using fossil fuel. Stability problems in the cells is another issue for commercial applications. To attain further improvement of the conversion efficiency of DSSCs, one of the important points is the improvement of the properties of nanoscale semiconductor oxide constituting of the titania electrode of DSSCs (Hagfeldt and Grätzel 2000; Law et al 2005). Titanium dioxide is the most promising material for the electrode of DSSCs. In this article, we present new findings on the morphology control, functionalization, and characterization of nanoscale titanium oxides, ie, network structure of single-crystal-like titania nanowires and titania nanorods, as well as their application for DSSCs.

Methods and materials

Formation of TiO_2 single crystalline network structure of nanowires

The procedure of TiO_2 single crystalline network structure of nanowires has been reported in our previous paper (Adachi et al 2004). In a typical synthesis process, laurylamine hydrochloride (LAHC) was dissolved in distilled water and tetraisopropylorthotitanate (TIPT) was mixed with acetylacetone (ACA) to decrease the

Correspondence: Motonari Adachi
Research Center of Interfacial Phenomena, Faculty of Engineering, Doshisha University, 1-3 Miyakodani, Tatara, Kyotanabe 610-0321, Japan
Tel +81 774 65 6420
Fax +81 774 65 6420
Email rca07002@mail.doshisha.ac.jp

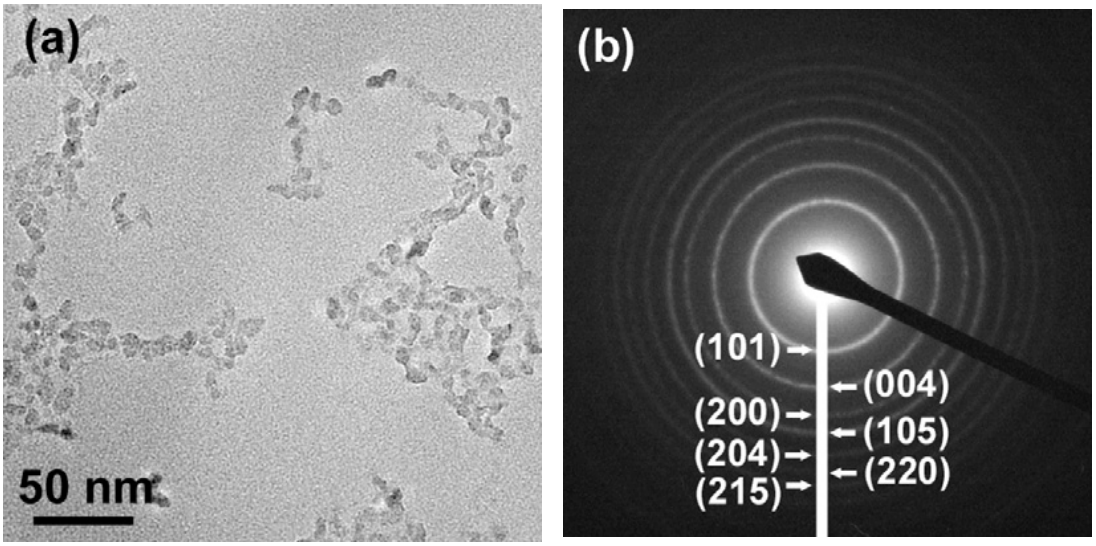

Figure 1 Single-crystalline-like network of TiO_2. (**a**) TEM image and (**b**) electron diffraction showing anatase.

hydrolysis and condensation rates of TIPT. When TIPT was mixed with the same molar ratio of ACA, ACA coordinated to the titanium atom, with one isopropoxyl group unbound. The coordination number of the titanium atom changed from 4 to 5, resulting in a color change from colorless to yellow. This yellow TIPT solution was added to 0.1 M LAHC aqueous solution (pH 4~4.5). The molar ratio of TIPT to LAHC was 4. When the two solutions were mixed, precipitation occurred immediately. The precipitates dissolved completely by stirring the solution for several days at 313 K, and the solution became transparent. The reaction temperature was then changed to 353 K. After three days, the solution became a white gel with a thin yellow liquid layer. The titania products were separated by centrifugation. After washing with 2-propanol and successive centrifugation, the titania powders were dried in a vacuum.

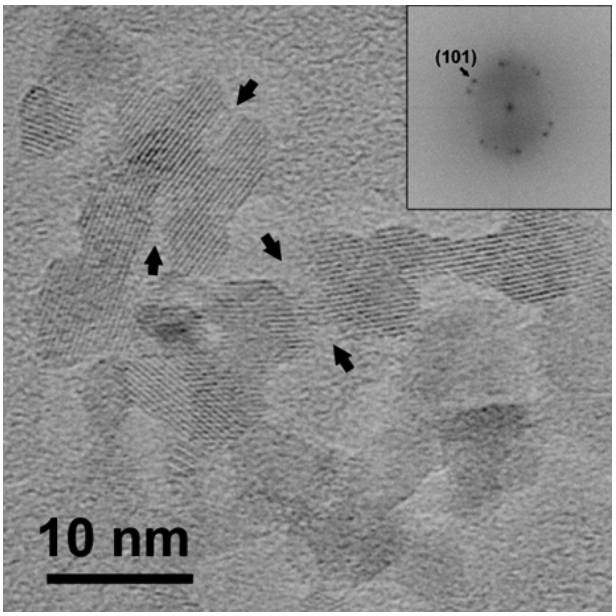

Figure 2. High resolution TEM image of fused TiO_2 particles. The inset shows the FFT of the image.

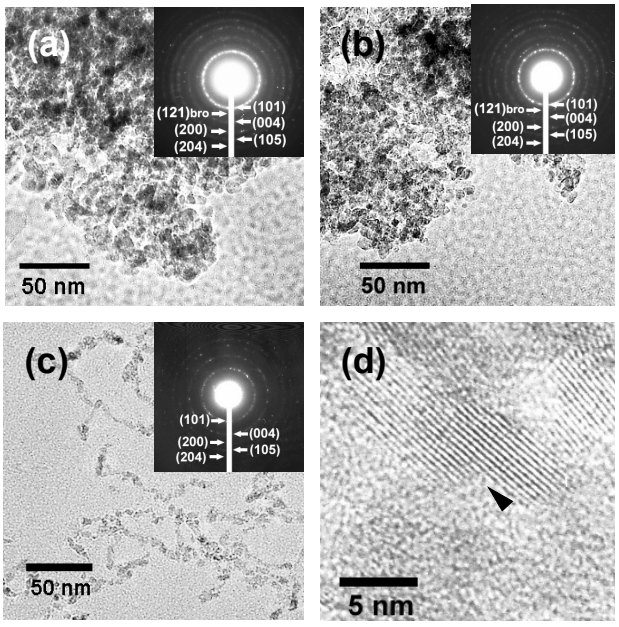

Figure 3 TEM images of TiO_2 nanostructures after reaction at 353 K for 4 days. (**a**) TIPT:ACA:LAHC = 4:0:0, inset: SAED patterns; (**b**) TIPT:ACA:LAHC = 4:0:1, inset: SAED patterns; (**c**) TIPT:ACA:LAHC = 4:4:0, inset: SAED pattern; (**d**) high resolution TEM image of (**c**).

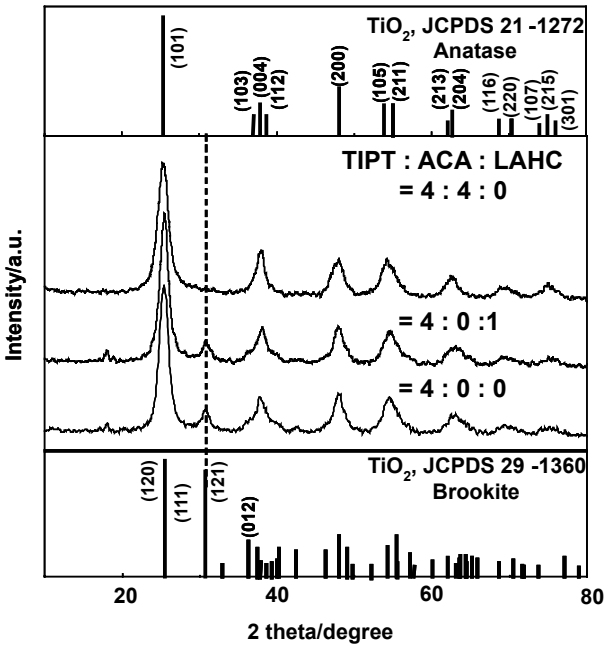

Figure 4 XRD patterns of TiO_2 nanostructures at TIPT:ACA:LAHC = 4:4:0, 4:0:1 and 4:4:0 after reaction at 353 K for 4 days.

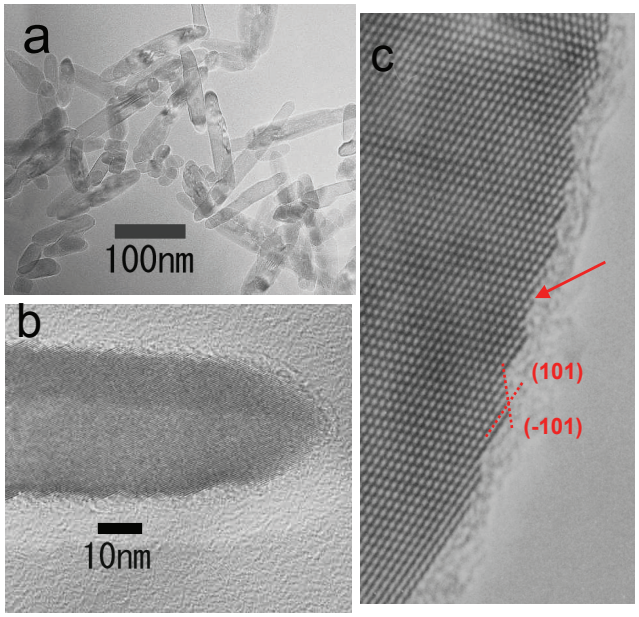

Figure 5 TEM images of high crystalline TR. (**a**) Low magnified image and (**b**) high magnified image. (**c**) High resolution image near the edge of TR.

Formation of highly crystallized TiO_2 nanorods

The procedure has been described in our previous paper. (Jiu et al 2006) Firstly 10 wt% aqueous solution of triblock copolymer of poly(ethylene oxide)$_{106}$-poly(propylene oxide)$_{70}$-poly(ethylene oxide)$_{106}$ (F127) containing 0.005 ~ 0.1 M cetyltrimethylammonium bromide (CTAB) was prepared at 308 K. After a transparent solution was obtained, TIPT (0.22 M) was added immediately into the above CTAB and F127 solution with stirring under ethylenediamine (EDA) basic catalyst. White precipitation obtained by hydrolyzation of TIPT was then transferred into a Teflon autoclave, sealed with a crust made of stainless steel, and reacted at 433 K for 6~12 h to nucleate and grow titania particles. The resulting white solid product was used for the formation of film electrode by adjusting the concentration of TiO_2 in the last suspension. In the experiment, we found the diameter and length of nanorod can be controlled by changing the mixing ratio of F127 to CTAB in the beginning, and these results will be discussed.

Characterization

Characterization of the produced materials was made by X-ray diffraction (XRD; Rigaku Goniometer PMG-A2, CN2155D2), transmission electron microscopy (TEM; JEOL 200 CX), fast Fourier transform (FFT), selected-area electron diffraction (SEAD), and isotherm of nitrogen adsorption (BEL SORP 18 PLUS). The photo-current-voltage characteristics were measured using an AM 1.5 solar simulator (ORIEL 1000W 91192 or Bunkoh-Keiki Co. Ltd., CEP-2000) in which the light intensity is 100 mW/cm^2. The cell size was 0.25 cm^2. The composition of electrolyte was 0.1 M of LiI, 0.6 M of 1,2-dimethyl-3-n-propylimidazolium iodide (DMPII), 0.05 M of I_2, and 0.5 M of 4-tert-butylpyridine (TBP) in methoxyacetonitrile.

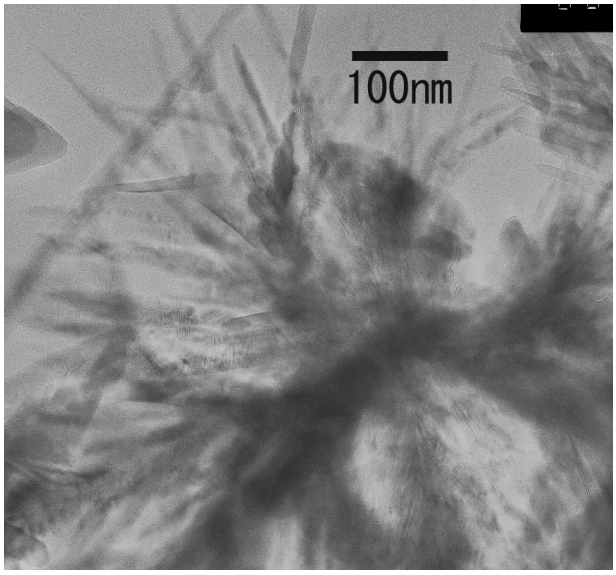

Figure 6 TEM image of slightly longer branched TiO_2 nanorods.

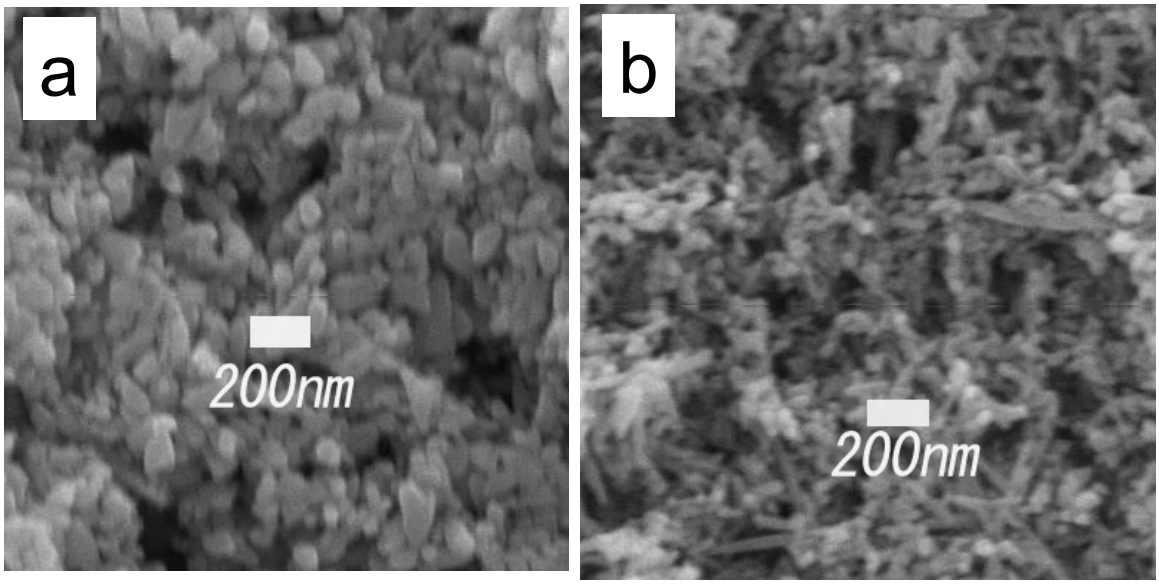

Figure 7 SEM images of nanorods films formed (**a**) without and (**b**) with F127 after calcination at 723 K.

Results and discussion

Figure 1a shows a TEM image of the vacuum-dried titania powders by heating at 353 K for 1 day. We can see the titania network consisting of nanowires with 5–15 nm in diameter. These titania nanowires (TW) have a very high crystalinity of anatase, as can be seen on an electron diffraction pattern (Figure 1b) in a wide area, showing the many Debye-Sherrer rings of (101), (004), (200), (105) and others of the anatase phase. A high resolution TEM image indicates again the high crystallinity of this system as shown in Figure 2 and besides a more interesting feature of this system. Most of the aggregated particles form a wire shape with a single-crystalline structure; there are almost no isolated particles observed. Lattice images are clearly observed running through particles, indicating that the nanowires are composed of fused nanoparticles with a diameter of 2–5 nm having high crystallinity in spite of their small size. Because the lattice image aligns perfectly, the orientation of crystals of fused nanoparticles are completely parallel. This feature shows that nanowires are made by an oriented attachment mechanism (Penn and Banfield 1999). A lattice spacing of 0.351 nm was determined by a FFT pattern (the inset of Figure 2) and corresponded to the lattice spacing of the {101} plane of the anatase phase.

This finding is very interesting because the crystal growth by the oriented attachment mechanism is observed below 373 K while usually much higher temperature is needed,

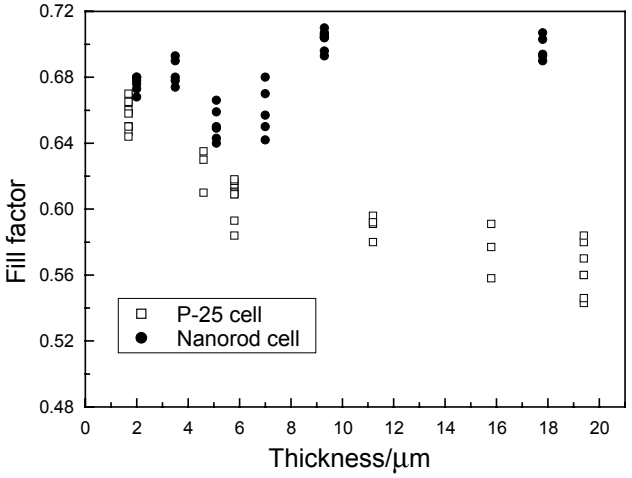

Figure 8 Fill factor of the cell composed of highly crystallized TR or P-25 vs film thickness.

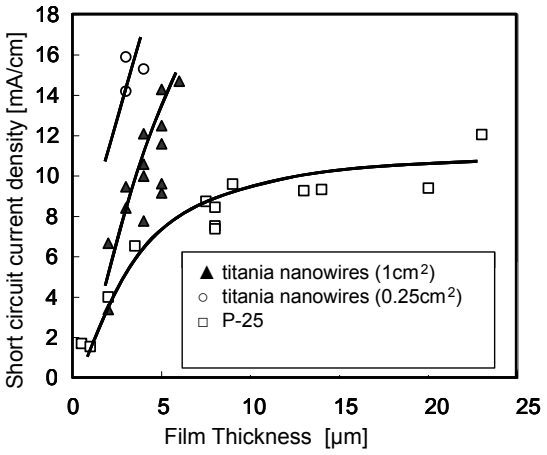

Figure 9 Shortcircuit current density of single-crystal-like TW or P-25 vs film thickness.

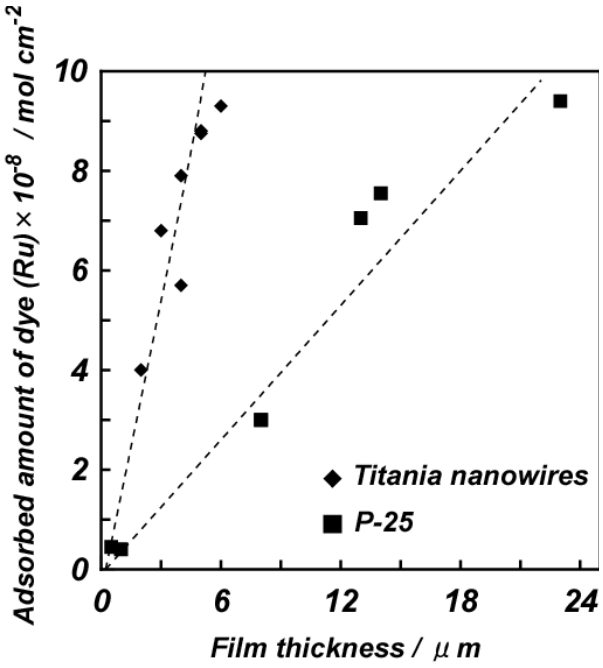

Figure 10 Adsorbed amount of dye for the cell composed of single-crystal-like TW or P-25.

ie, 433–523 K (Penn and Banfield 1999). This observation confirmed a remarkable characteristic of this surfactant-assisted synthesis method using ACA. In this synthesis, two reagents were added to the TIPT solution, that is, LAHC and ACA. In order to examine the roles of these reagents, three samples with mole ratio at TIPT:ACA:LAHC = 4:0:0, 4:0:1 and 4:4:0 were synthesized. When TIPT:ACA:LAHC was 4:0:0 and 4:0:1, white colloidal suspensions were formed immediately after mixing of two reactants. Figure 3 shows the TEM images and the selected area electron-diffraction (SAED) patterns of the gel samples at the different mole ratio of TIPT:ACA:LAHC after reaction at 353 K for 4 days. When TIPT:ACA:LAHC was 4:0:0 and 4:0:1, gelation did not occur. Nanoparticles with diameter of 8–10 nm are observed as shown in Figures 3a and 3b. Both SAED patterns show the Debye-Scherrer rings which can be indexed to those of anatase phase and (121) diffraction of brookite phase of TiO_2. On the contrary, when TIPT:ACA:LAHC was 4:4:0, gelation occurred after reaction at 353 K. Nano-network structure connecting nanowires with diameter 6–9 nm was observed, and SAED pattern showed only anatase phase as shown in Figure 3c. A high resolution TEM image of this nano-network structure is shown in Figure 3d. Clear lattice image of (101) plane of anatase phase was aligned over several particles, which indicates that the "oriented attachment" occurred under this condition.

Figure 4 shows the XRD (Rigaku RAD-IIC) patterns of TiO_2 nanostructures after reaction at 353 K for 4 days. The peaks of nanostructures at TIPT:ACA:LAHC = 4:0:0 and 4:0:1 could be indexed to anatase phase (JCPDS file

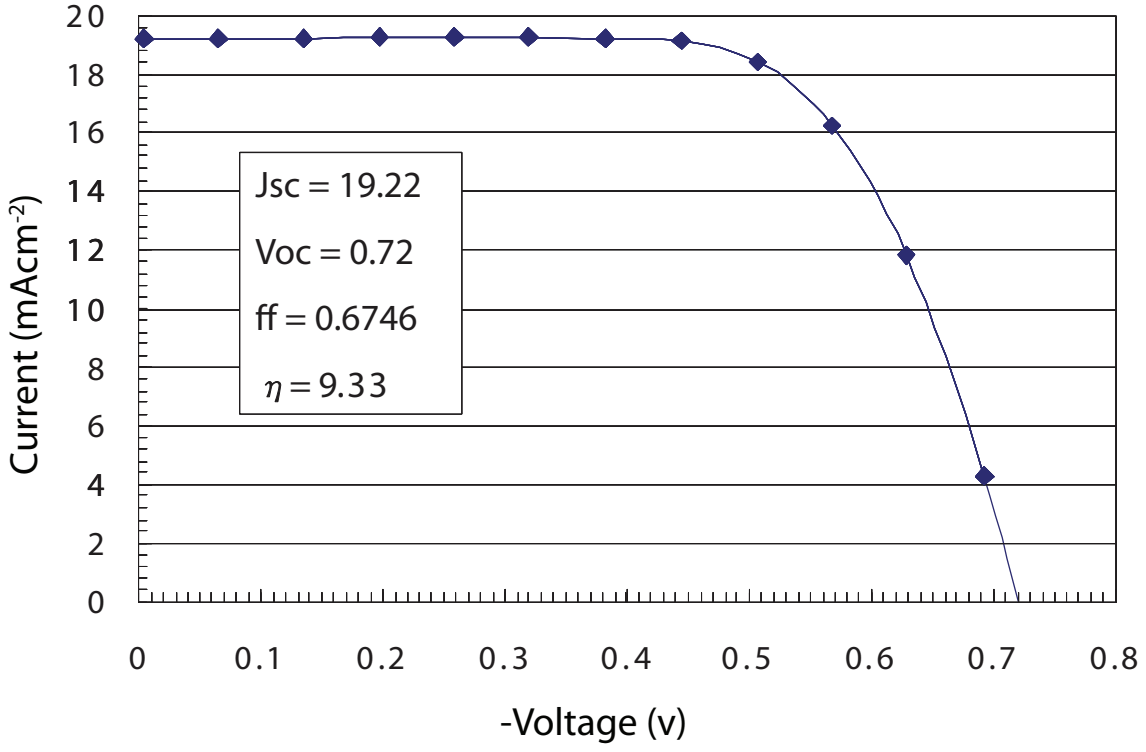

Figure 11 I-V curve obtained for the cell composed of single-crystal-like TW.

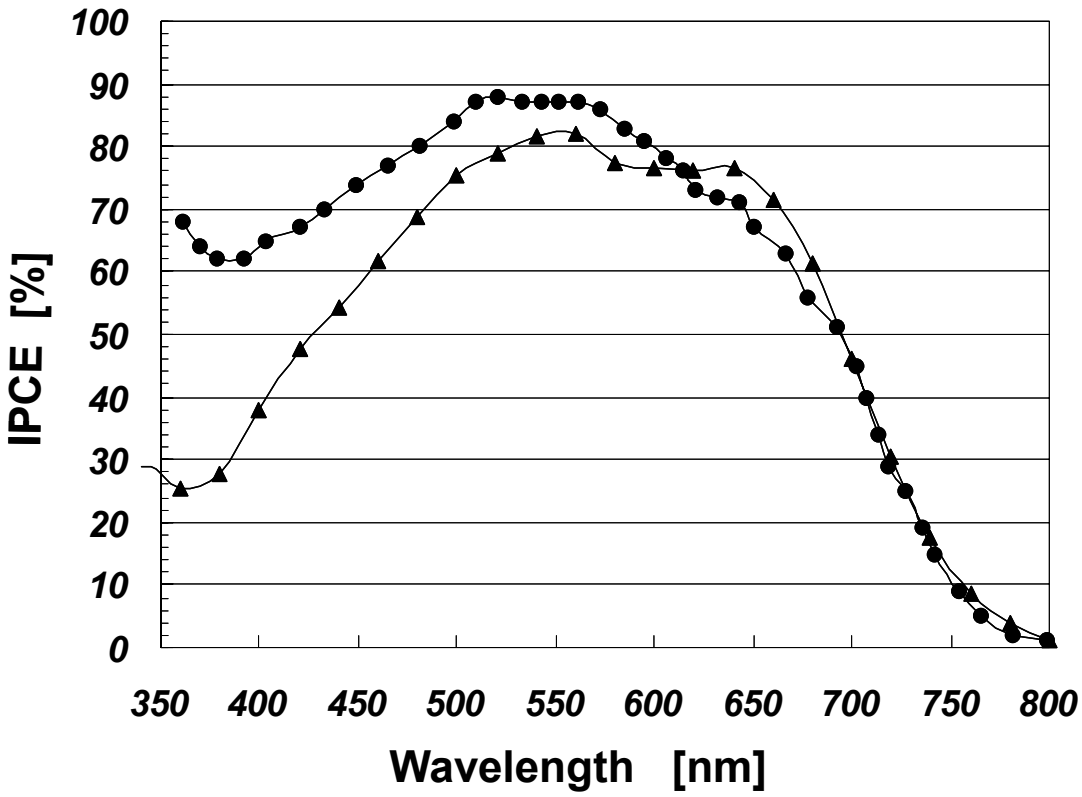

Figure 12 IPCE obtained for the cell shown in Figure 11 (triangle), together with the result reported by Grätzel (2005) (solid circle).

no. 21-1272) and (121) diffraction of bookite phase of TiO_2 (JCPDS file no. 29-1360). However, the peaks at TIPT:ACA:LAHC = 4:4:0 could be indexed to only anatase phase. These results coincide with the results of TEM images and SAED patterns. In addition, an increase in the peak height ratio of (004)/(200) and a sharpening of the (004) peak are observed, which indicates the presence of nanocrystalline anatase with a typical anisotropic growth pattern along the [001] direction.

Acetylacetone has often been used in sol-gel processing as a chemical additive to reduce the reactivity of metallic alkoxides. The binding of ACA to titanium decreases the reactivity. The decrease in reaction rates might enable the occurrence of the oriented attachment, because nanoparticles produced by reaction of TIPT have enough time to select the crystalline face to fuse with each other. TiO_2 can select most stable structure when they react with nanocrystals. Thus, it is revealed that ACA plays an important role of not only making hydrolysis and condensation reactions slow, but also controlling the morphology and crystalline structure of TiO_2.

Highly crystallized titania nanorods (TR) have been synthesized by hydrothermal process using blockcopolymer (F127) and surfactant cetyltrimethylammonium bromide (CTAB) as a mixed template. Figure 5a shows a typical TEM image of the obtained TR with 100–300 nm in length and 20–30 nm in diameter. A high resolution TEM image of single TR shows clear lattice fringes (Figure 5b), indicating that the nanorods exhibit high crystallinity with few structual defects. The fringes are {101} planes of anatase TiO_2 with a lattice spacing of about 0.351 nm. The long direction of the nanorod is along the [001] direction. A highly magnified high resolution TEM image (Figure 5c) shows that the surface of TR is facetted with the TiO_2 anatase {101} faces as shown by lines in the fringe.

When F127 was not used, the formation of slightly longer branched TiO_2 nanorods was observed with diameter of 20–30 nm and lengths of 500 nm before calcination (TEM images in Figure 6). As shown by SEM images in Figure 7, however, the TR formed without F127 changed into smaller granular particles after calcination at 723 K for 1 h. On the other hand, the TR synthesized with F127 kept its original rod shape well even after the same calcination. Moreover, it was confirmed that the shape of TR is reserved even after calcination at higher temperature of 823 K, and then F127 surfactant is essential to keep the rod-shape for application to DSSC through calcination.

The highly crystallized TR and the single-crystalline-like network structure of nanowires mentioned above provide one

dimensional highly crystallized TiO_2 materials, which are expected to improve the electron transport properties in TiO_2 electrode of DSSCs. Usually a porous thin film composed of titania nanosize particles to achieve a high specific surface area for adsorption of a large number of dye molecules. However, the electron diffusion coefficients determined by laser flash-induced transient photocurrent measurement (Solbrand et al 1997; Kopidakis et al 2000; Kambe et al 2002; Nakade et al 2001) and intensity modulated photocurrent spectroscopy (Dolczik et al 1997; Fisher et al 2000) were more than three orders of magnitudes smaller than the value for bulk anatase crystal. These small diffusion coefficients can be simply understood by the hypothesis of probable electron traps in the porous TiO_2 with a very broad distribution of release rate. Defects in the porous TiO_2 may act as electron traps at the grain boundaries of the contacts between nanosize particles. Thus, the use of one dimensional highly crystallized TiO_2 nanomaterials instead of TiO_2 nanoparticles is convinced to result in rapid electron transfer, that is, higher efficiency.

Figure 8 shows the fill factor of the cell composed of highly crystallized TR or P-25. The fill factor relates closely with the total internal resistance of the cell. Though the results show that the fill factor for P-25 decreases with increasing thickness of TiO_2 electrode, the fill factor for TR keeps almost constant value regardless of the thickness of the film, supporting the above anticipation. A high light-to-electricity conversion efficiency of 7.0%–7.3% was obtained using a Bunkoh Keiki solar simulator. On the other hand, a solar cell made of network of single-crystalline anatase nanowires shows two remarkable characteristic properties. A cell made of those nanowires gives the high current density in the thin film region as shown in Figure 9 in comparison with that of P-25 cell. The second point is that the amount of N3 dye adsorbed by the titania network of nanowires is about four times higher than that of P-25 film for the same film thickness (Figure 10). Figure 11 shows the current-voltage characteristics obtained for a cell with the TiO_2 thin film composed of the network structure of single-crystalline anatase nanowires under AM 1.5 100 mW/cm^2. A high light-to-electricity conversion rate of 9.3% was obtained using an Oriel solar simulator. The IPCE result of this DSSCs is demonstrated in Figure 12, together with the result reported by Grätzel and colleagues (Nazeeruddin et al 1993), confirming the high light-to-electricity conversion yield of the cell.

Conclusion

A titania nanonetwork structure composed of single-crystal-like anatase nanowires was successfully synthesized by a surfactant-assisted "oriented attachment" mechanism at a low temperature of 353 K. Also, we succeeded in the formation of a single crystalline anatase TiO_2 nanorods by a surfactant-assisted hydrothermal method. A high resolution TEM image of single titania nanorods shows clear lattice fringes, indicating that the nanorods exhibit high crystallinity with a few defects. A high light-to-electricity conversion yield of 9.3% was achieved by applying the titania nanonetwork structure of single-crystal-like anatase nanowires as the titania thin film of dye-sensitized solar cells.

Disclosure

The authors report no conflicts of interest in this work.

References

Adachi M, Murata Y, Takao J, et al. 2004. Highly efficient dye-sensitized solar cells with a titania thin-film electrode composed of a network structure of single-crystal-like TiO_2 nanowires made by the "oriented attachment" mechanism. *J Am Chem Soc*, 126:14943–9.

Chiba Y, Islam A, Watanabe Y, et al. 2006. Dye-sensitized solar cells with conversion efficiency of 11.1%. *Jpn J Appl Phys*, 45:L638–L640.

Dloczik L, Ileperuma O, Lauermann I, et al. 1997. Dynamic response of dye-sensitized nanocrystalline solar cells: Characterization by intensity-modulated photocurrent spectroscopy. *J Phys Chem B*, 101:10281–9.

Fisher AC, Peter LM, Ponomarev EA, et al. 2000. Intensity dependence of the back reaction and transport of electrons in dye-sensitized nanocrystalline TiO_2 solar cells. *J Phys Chem B*, 104:949–58.

Grätzel M. 2004. Conversion of sunlight to electric power by nanocrystalline dye-sensitized solar cells. *J Photochem Photobio A Chem*, 164:3–14.

Grätzel M. 2006. Photovoltaic performance and long-term stability of dye-sensitized meosocopic solar cells. *C R Chimie*, 9:578–83.

Grätzel M. 2005. Solar energy conversion by dye-sensitized photovoltaic cells. *Inorg Chem*, 44:6841–51.

Hagfeldt A, Grätzel M. 2000. Molecular photovoltaics. *Acc Chem Res*, 33:269–77.

Jiu J, Isoda S, Wang F, et al. 2006. Dye-sensitized solar cells based on a single-crystalline TiO_2 nanorod film. *J Phys Chem B*, 110:2087–92.

Kambe S, Nakade S, Kitamura T, et al. 2002. Influence of the electrolytes on electron transport in mesoporous TiO_2-electrolyte systems. *J Phys Chem B*, 106:2967–72.

Kopidakis N, Scjiff A, Park N-G, et al. 2000. Ambipolar diffusion of photocarriers in electrolyte-filled, nanoporous TiO_2. *J Phys Chem B*, 104:3930–6.

Law M, Green L, Johnson JC, et al. 2005. Nanowire dye-sensitized solar cells. *Nature Mater*, 4:455–9.

Nakade S, Kambe S, Kitamura T, et al. 2001. Effects of lithium ion density on electron transport in nanoporous TiO_2 electrodes. *J Phys Chem B*, 105:9150–2.

Nazeeruddin MK, Kay A, Rodicio I, et al. 1993. Conversion of light to electricity by cis-X2bis(2,2'-bipyridyl-4,4'- dicarboxylate) ruthenium(II) charge-transfer sensitizers (X = Cl-, Br-, I-, CN-, and SCN-) on nanocrystalline titanium dioxide electrodes. *J Am Chem Soc*, 115:6382–90.

Penn RL, Banfield JF. 1999. Morphology development and crystal growth in nanocrystalline aggregates under hydrothermal conditions: insights from titania. *Geochimica Cosmochimica Acta*, 63:1549–57.

Solbrand A, Lindstrom H, Rensmo H, et al. 1997. Electron transport in the nanostructured TiO_2-electrolyte system studied with time-resolved photocurrents. *J Phys Chem B,* 101:2514–18.